

A Robust Approach to Automatic Groove Identification in 3D Bullet Land Scans

Kiegan Rice, M.Sc., Heike Hofmann, Ph.D., Ulrike Genschel, Ph.D.

Abstract

Forensic firearms examiners analyze bullets through a process of visual feature comparison to determine whether two bullets originate from the same source. Striation marks found on land engraved areas (LEAs) provide evidence to address this same source-different source problem. Advances in technology have led to an increase in research focused on applying image-analysis algorithms to the automated, quantitative analysis of bullet evidence. One prominent example is an algorithm developed by [Hare et al., 2017] based on 3D imaging data of LEAs. This algorithm relies on removal of the overall curve of the bullet to obtain what [Hare et al., 2017] refer to as a “signature”. Cross-correlation functions, consecutive matching striae, consecutive non-matching striae and other features are then calculated based on pairwise comparisons of these signatures. The currently established best practice for collection of 3D images of bullet LEAs requires capturing portions of the neighboring groove engraved areas (GEAs). Analyzing LEA and GEA data separately is imperative to achieve high accuracy and precision in subsequent feature calculations. However, existing standard statistical modeling techniques fall short when applied to the atypical structure of 3D bullet data, often failing to adequately separate LEA and GEA data. We propose a method based on robust locally weighted regression and show that this method outperforms current methods at separating LEA and GEA data.

Contents

1	Background	1
2	Data Source	3
3	Methodology	4
3.1	Robust Linear Models	5
3.2	Robust LOESS	7
4	Results	9
5	Conclusions	11
6	References	11

TODO: -Kiegan, could you use a color label, so I can see the changes you made in the file rather than as commit message? - I’ve made a kr command for you - you can pick the color :) - done!

- Could you remove the derivative files (tex, blg, writeup_files, ...) from the repo? They cause a ton of merge conflicts. - done!
- I can’t find the code for figure groove_vs_nogroove.png - I would like to split the figure into two subfigures (top) and (bottom) with extra lines of labelling options - I’ve updated it to be a generated plot! I didn’t make any labelling changes yet.
- replace the * multiplication by cdot or times - done!

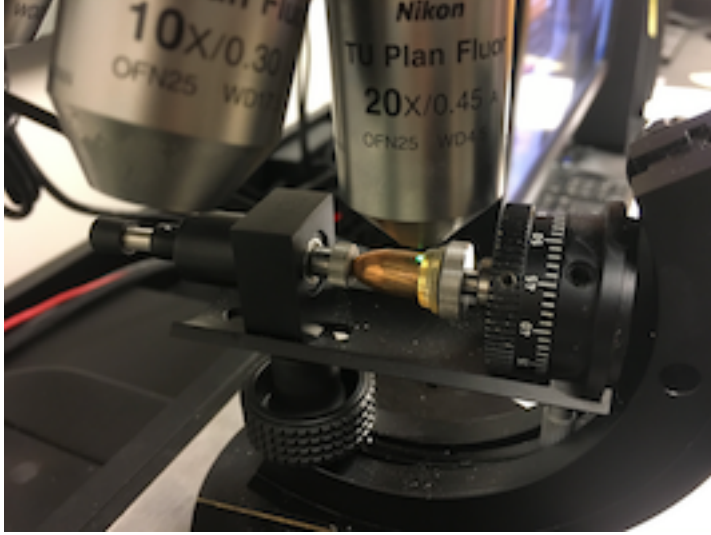


Figure 1: Collection of data from the surface of a bullet. Other image H44 B1 B1 L2 will go here.

1 Background

Forensic firearms examiners analyze bullets through a process of visual feature comparison to determine whether two bullets originate from the same source. Two bullets in question are placed under a comparison microscope and firearms examiners evaluate similarities and differences between the bullets’ striation marks according to the AFTE Theory of Identification [AFTE Glossary, 1998] guidelines resulting in a decision about whether both bullets were fired through the same gun barrel. In forensic science, this problem is known as the same source-different source problem and focuses on establishing quantitative evidence whether two bullets were fired through the same gun barrel.

Recent advances in technology, particularly wider access to high resolution 3D microscopy tools, have led to an increase in research focused on image-analysis algorithms for automated, quantitative analyses of bullet evidence. The introduction of this scanning technology to the field of forensic science allows for capture of high resolution 3D images of bullet LEAs, depicted in Figure 1 [see De Kinder et al., 1998, De Kinder and Bonifanti, 1999, Bachrach, 2002]. The resulting 3D images have since been used in the development of several methods for automated comparison of land engraved areas [e.g. Ma et al., 2004, Chu et al., 2010, 2013, Hare et al., 2017]. [Make sure to reference the image somewhere in here.](#)

In this paper, we will focus only on barrels with traditional sharp-edged lands and grooves (i.e., no polygonal rifling). Sections of the bullet that make the closest contact with the barrel are called land engraved areas (LEAs). Those alternate with groove engraved areas (GEAs). Microimperfections in the barrel introduce striae on the bullet during the firing process. The resulting striation marks provide evidence to address the same source-different source problem. A guiding principle in forensic firearms analysis is that two bullets fired through the same barrel will bear more similar striation marks on their LEAs than two bullets fired from different barrels. Hare et al. [2017] proposes a matching algorithm based on 3D imaging data of LEAs. Horizontal slices of the 3D images, called profiles, provide a detailed representation of striae impressed on the surface at a horizontal cross-section of each LEA. A current limitation of this algorithm is that it can not deal with a mix of striae from both LEA and GEAs. For the human visual system, separating the two areas is straightforward. However, the same cannot be said for automated computer vision techniques.

A correct identification of LEAs is vital to achieve high accuracy and precision in the subsequent downstream analysis. The purpose of this paper is to discuss different automated methods for identifying so-called shoulder locations, the locations at which the land engraved areas end and the groove engraved areas begin.

The structure of the paper is as follows: ...

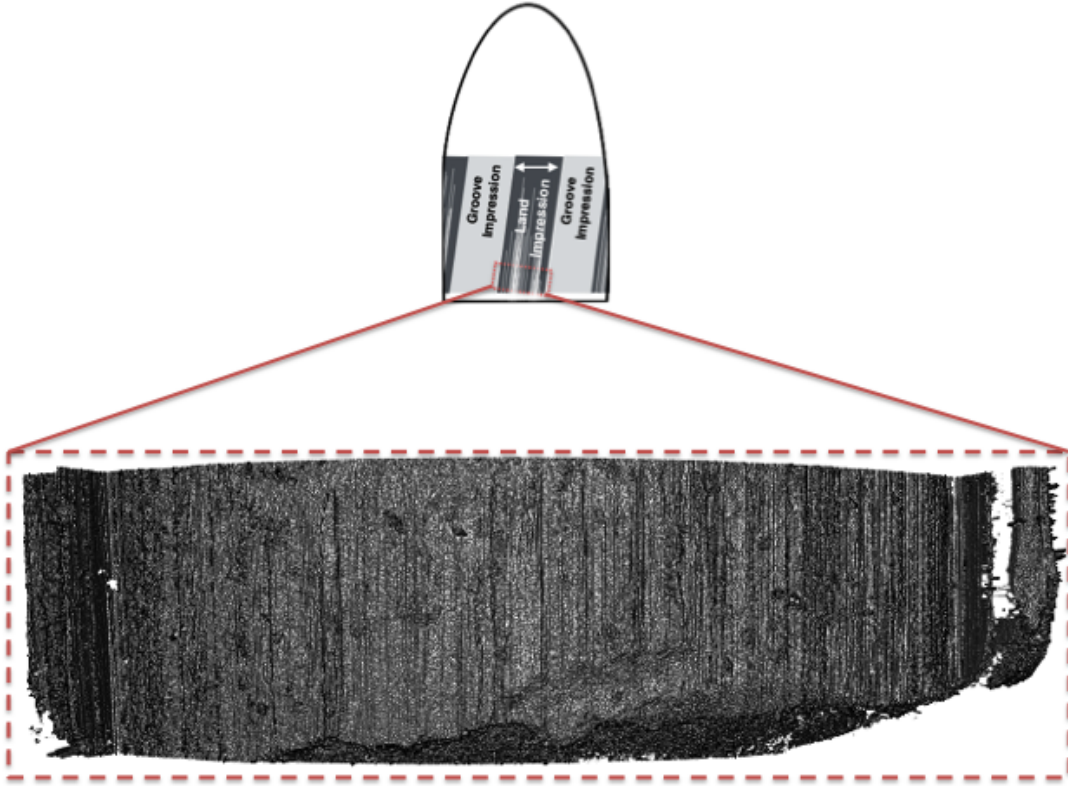


Figure 2: Visualization of 3D data collected through high resolution scanning of a land engraved area. Striations on the surface of the object can be seen by viewing this data from "above", as presented here.

2 Data Source

All currently published automated methods rely on high resolution 3D scans of bullet land engraved areas. Currently accepted best practice for collecting 3D images of bullet LEAs requires that bullets are staged such that striae appear vertically in the scan. Scanning across the LEA must begin and end in the neighboring groove engraved areas as shown in Figure 2. Parts of the breakoff are captured as a visual reference for orientation.

Scans are exported from the microscope as x3p files, conforming to the ISO5436-2 standard [ISO 5436-2:2012, en]. Each scan is captured as a matrix of (x, y) locations with a measured relative height value z recorded for each (x, y) location on the LEA.

The algorithm proposed by Hare et al. [2017] uses so-called crosscuts, height measurements along x for a fixed y . Removal of the overall curve of the bullet – the global structure captured in the 3D scanning process – transforms these profiles into to what Hare et al. [2017] refer to as signatures (see Figure 3). The assessment of similarity between two LEAs is then based on a set of extracted features such as cross-correlation function, number of consecutively matching striae [see Biasotti, 1959] and maximum number of consecutively non-matching striae. Successful extraction of this set of features depends on how well we can remove the global bullet structure to translate from a crosscut to the corresponding signature.

In this paper, we are introducing and comparing two methods for identifying shoulder locations. In order to

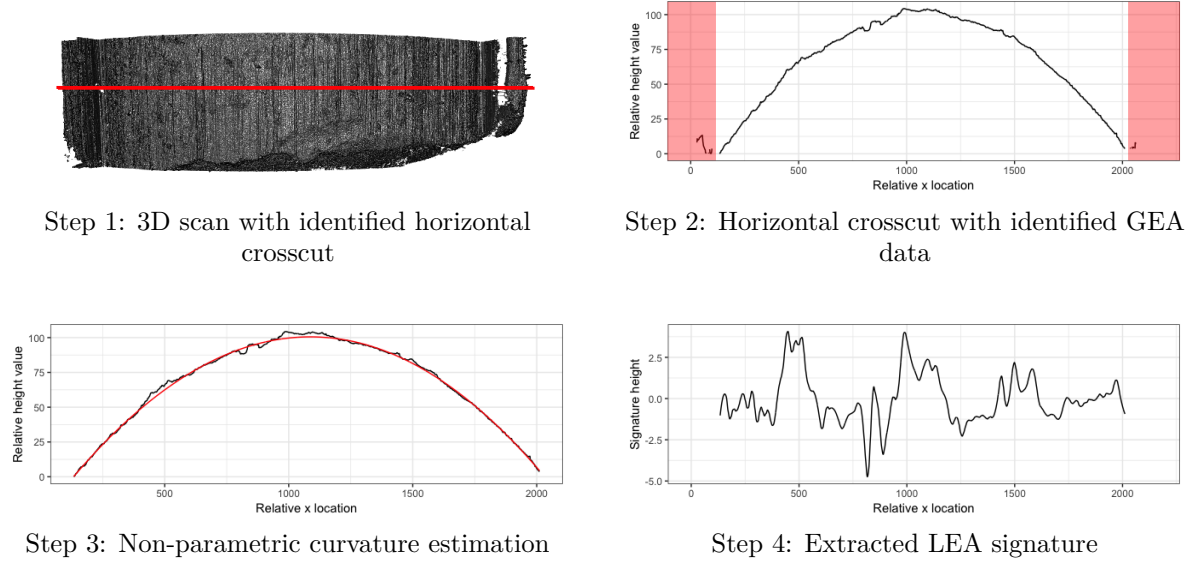


Figure 3: The process of extracting a 2D signature from a 3D LEA scan described by Hare et al. [2017]. GEA removal between Step 2 and Step 3 is critical to ensure precise signature extraction. UPDATE TO BE PROMINENT GEAs. ADD ZERO LINE TO SIGNATURE.

to assess the performance of these methods, we are applying the methods on 3D scans of LEAs from Hamby set 44 [Hamby et al., 2009]. Each Hamby set consists of 35 bullets fired from 10 consecutively rifled Ruger P85 barrels.

Each fired bullet in Hamby Set 44 has 6 LEAs; every LEA was scanned for each of the 35 bullets, producing data for 210 individual lands. Two lands – Barrel 9, Bullet 2, Land 3 and Questioned Bullet L, Land 5 – were removed from consideration due to “tank rash”. Tank rash results from a bullet striking the bottom of a water recovery tank after exiting the barrel, thereby creating marks on the land that are not due to the contact with the barrel.

The 3D scans of Hamby Set 44 were captured at Iowa State University’s Roy J. Carver High Resolution Microscopy Facility with a Sensofar Confocal light microscope at 20x magnification resulting in a resolution of 0.645 microns per pixel. Physically, each land is approximately 2 millimeters in width; as such, data structures for a single LEA can contain more than 3 million individual data points.

The data used to assess performance of the two methods consists of 2D crosscuts gathered from the 3D scans, as shown in Figure 4.

3 Methodology

The structure in the 2D crosscuts is dominated by the curvature of the physical object (the bullet). To assess the similarity of features from two land engraved areas, this curvature has to be removed.

Non-parametric methods suggested in the literature, such as a LOESS fit [Hare et al., 2017] or a Gaussian filter [Chu et al., 2010] are very effective for removing the curvature to extract a signature. However, they are prone to boundary effects, which are mischaracterizations of data patterns near the boundaries of the data domain. In the case of crosscuts, the boundaries are often dominated by values originating from the GEA structure. This structure exaggerates existing boundary effects because GEAs introduce a secondary structure different from the main curvature of the LEA. This can be seen in both Figure 4 and Figure 5. Figure 4 shows how much a non-parametric LOESS fit is affected by including GEA data. Figure 5 shows the effect this same inclusion has on extracted signatures. If included, GEA data result in strong boundary effects

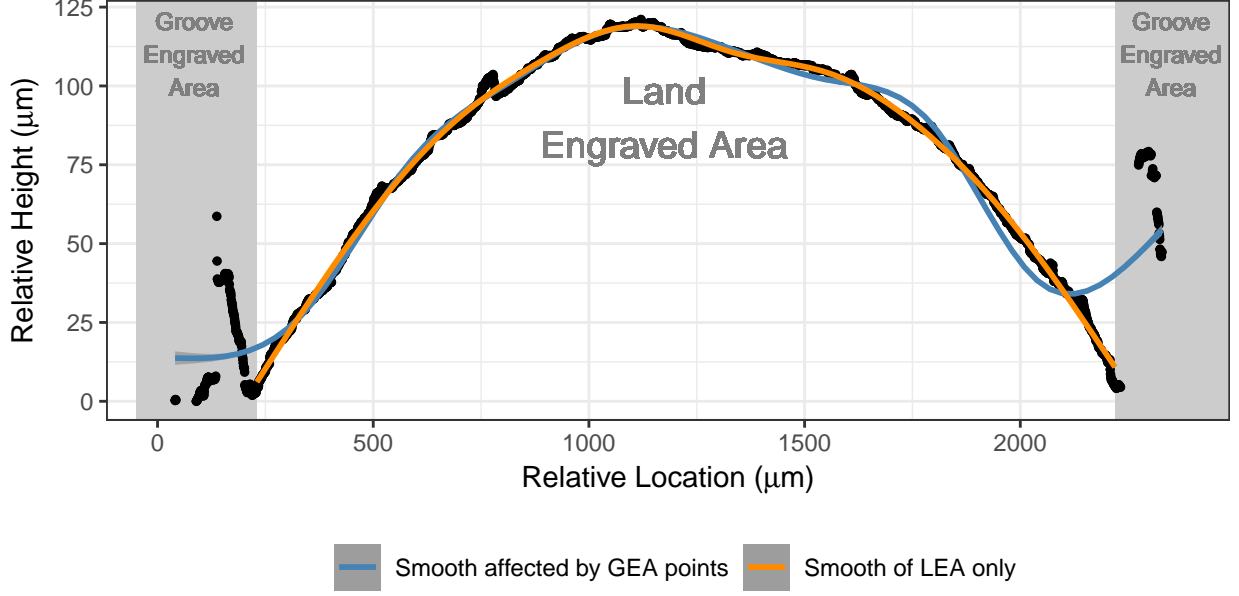


Figure 4: The black points show measured heights for a single crosscut of a 3D LEA scan. The main data structure, located in the center, is comprised of the land engraved area. The groove engraved areas are found on the left and right sides of the crosscut. The lines show fits of two non-parametric LOESS smooths, with and without GEA data. When GEA data is included, the smooth fails to estimate the main LEA structure near the boundaries.

in the signatures. Statistically, the GEA data introduces outliers into the LEA data. In the next sections, we introduce two methods for fitting the LEA structure. Both methods aim to describe the relationship between horizontal position and relative height on a crosscut. While the two approaches differ in methodology, they are both rooted in the ability to mitigate influence caused by outlying data.

In the following, we will describe the horizontal position on a crosscut of a scan as x_i and measured relative height as z_i , where $i = 1, \dots, n$, the number of data points along a crosscut.

3.1 Robust Linear Models

A natural candidate for a curved structure is a quadratic linear model of the form

$$z_i = \beta_0 + \beta_1 x_i + \beta_2 x_i^2 + \epsilon_i,$$

where $\epsilon_i \stackrel{iid}{\sim} N(0, \sigma^2)$ is the error term.

Quadratic linear models fit by finding the values of $\beta_0, \beta_1, \beta_2$ which minimize:

$$\arg \min_{\beta} \sum_{i=1}^n (z_i - (\beta_0 + \beta_1 x_i + \beta_2 x_i^2))^2,$$

the vertical squared distance between each measured height value and a fitted quadratic line. Figure 6 shows that the presence of unusual data near the boundaries pulls the fitted curve upwards towards GEA data.

An alternative approach is a robust linear model which minimizes absolute deviations in place of squared deviations:

$$\arg \min_{\beta} |z_i - (\beta_0 + \beta_1 x_i + \beta_2 x_i^2)|.$$

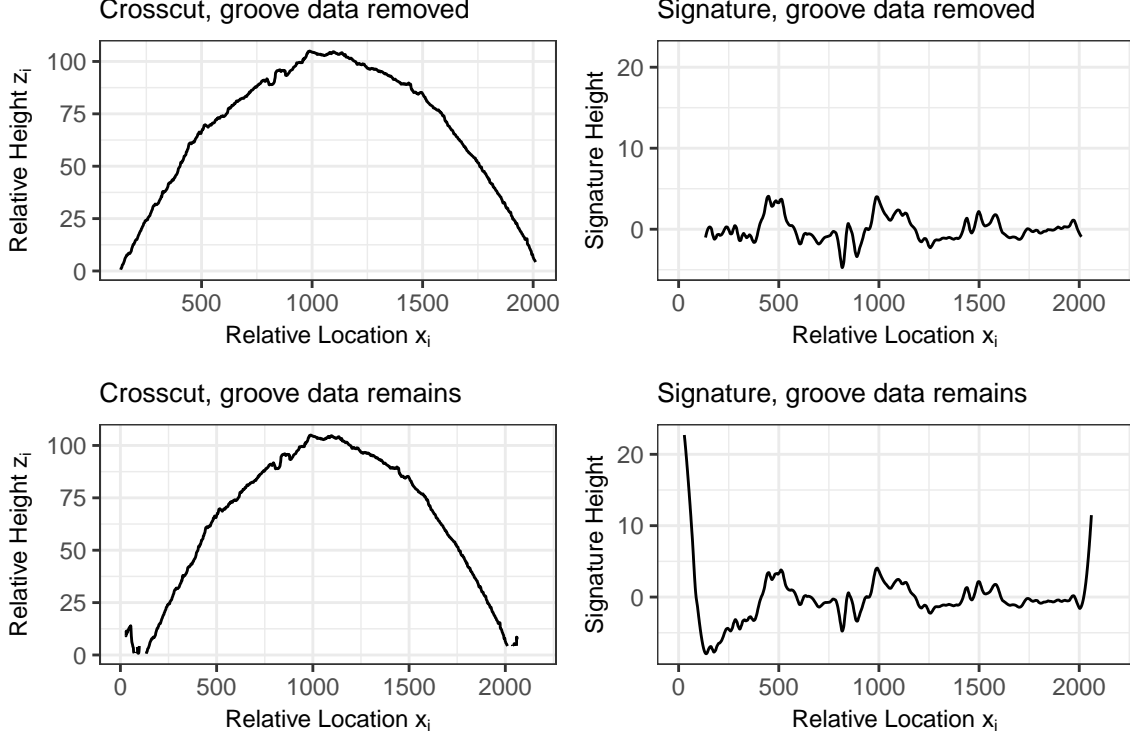


Figure 5: An example of the impact failure to remove GEA data can have on an extracted 2D signature. The extracted signatures are dominated by boundary effects introduced by remaining GEA structure.

This method of minimization is less influenced by large outlying values present in the GEA data. The vast majority of data points are in the LEA structure; minimization of absolute deviations favors fitting the majority structure closely and allows the minority structures on the edges to have high residual values. Prioritization of the majority structure is here preferable to the compromise that occurs in traditional linear models due to minimizing the squared distance. A striking example of the difference in results from these two model frameworks is seen in Figure 6, where the fit of a linear model compromises between the LEA and GEA structures, and fails to fit either structure appropriately.

The focus on closely fitting majority structure results in residual values scattered near zero in the LEA and larger, mostly positive residuals in the GEA zones. Thus, the magnitudes of residuals can serve as an indicator of membership as LEA data or GEA data. More precisely we define the median absolute deviation (MAD).

The MAD is a robust metric for the spread of points, similar to the standard deviation. It is preferable to the standard deviation to quantify the spread since we are dealing with an unbalanced spread of residual values. Let m be the median:

$$MAD(\mathbf{z}) = m(|z_i - m(\mathbf{z})|) \quad \forall z_i \in \mathbf{z}.$$

Reduce the next paragraph to 2 sentences done - I think!

Residual values that are considered unusually high, or outlying, are values that are larger than $4 \times MAD$. Any residual value larger than 4 times the median absolute deviation value is defined to be a “large” residual and is likely a member of the GEA structure.

what does it mean to be a large residual? Nail your point!

Shoulder location predictions are calculated for each profile in the following manner:

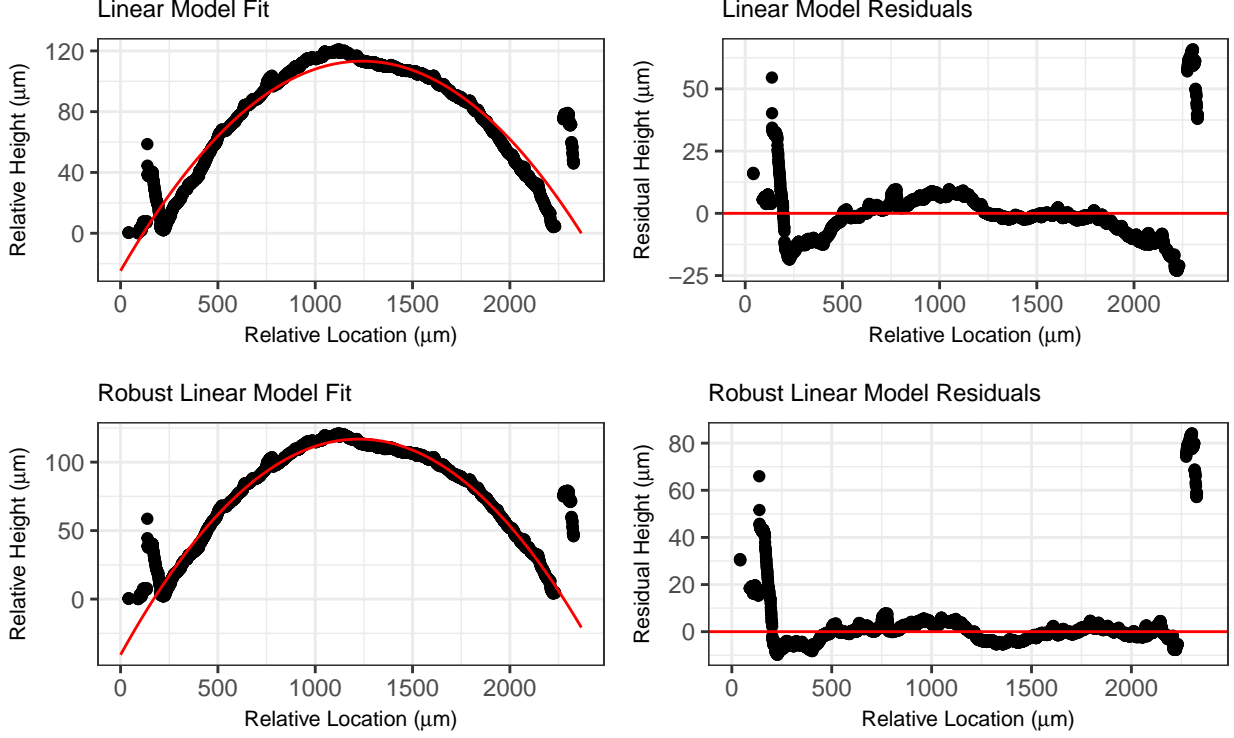


Figure 6: Example of a quadratic linear model fit and resulting residuals (top) compared to a robust quadratic linear model fit and residuals (bottom) for a single profile. The robust model is able to more effectively capture the curved structure of the LEA without being influenced by the GEA.

1. Fit a robust linear model of order 2 (i.e., quadratic) to the averaged profile.
2. Calculate a residual value for each data point on the profile.
3. Calculate the median absolute residual (MAD) for the profile.
4. Remove all data points on the profile whose absolute residual value is greater than $4 \times \text{MAD}$.
5. Identify the range of the remaining x values - these are the predicted shoulder locations for that profile.

3.2 Robust LOESS

Locally weighted regression, known as LOESS, is a non-parametric approach that is not restricted by the need for perfect quadratic curvature. This is advantageous when working with bullets, as it is unrealistic to expect a flawless circular shape to remain after the bullet has been subjected to the forces of a gun barrel and striae have been impressed upon it.

LOESS models estimated a predicted value for each z_i height by finding the values of β_0, β_1 which minimize:

$$\arg \min_{\beta} \sum_{k=1}^n w_k(x_i) (z_k - (\beta_0 + \beta_1 x_k))^2,$$

which assigns a weight $w_k(x_i)$ to each data point with index k based on its proximity to the x_i of interest. Weights w_k decrease as the proximity to x_i decreases, so that the data points closest to x_i of interest influence the prediction of z_i most. This can also be described as a non-parametric weighted average of many parametric models fit to subsets of the data.

This approach allows for greater flexibility. However, it also means that LOESS models are affected by GEA structures in a more unpredictable manner. Data points near and in the GEA structure will be most influenced by other GEA data rather than the overall global structure seen in LEA data. This results in a set of predictions which misrepresents much of the data near one or both boundaries (see Figure 7).

This next paragraph would be gone:

LOESS fits many models to small subsets of the data and combines them into one non-parametric fit of the data, rather than focusing on the overall structure of the data. This allows for greater flexibility. However, it also means that LOESS models are affected by GEA structures in a more unpredictable manner. A model fitted on a subset of data that mainly falls in the GEA structure can look very different than a model fit with data from the LEA. This results in a combined prediction that misrepresents much of the data near one or both boundaries (see Figure 7).

XXX.

The robust approach to LOESS uses an iterative re-weighting process to reduce the influence of outlying data points [see @Cleveland1]. First, an initial LOESS is fit. This is followed by a redistribution of $w_k(x_i)$ values based on residual values, $e_i = (z_i - \hat{z}_i)$. New weights are calculated as

$$\left(1 - \left(\frac{e_k}{6 \times MAD}\right)^2\right)^2 \times w_k(x_i) \quad \text{if } \left|\frac{e_k}{6 \times MAD}\right| < 1.$$

Otherwise, weights are set to 0. These new weights are applied and updated predictions are calculated. This reduces the influence of data points which have large values of e_k in the first LOESS iteration. In the LEA profile context, it reduces the influence of GEA data.

The above would replace the next paragraph.

Robust LOESS utilizes an iterative process focused on re-weighting [see Cleveland, 1979]. First, an initial LOESS fit is created. This is followed by a step which gives smaller weights to data points with high residual values, and a subsequent LOESS fit with new weights applied. The down-weighting of values with high residual values slowly reduces the influence of the GEA data. This iterative process results in a non-parametric fit to the LEA structure that treats GEA data as less important, which is desirable.

While robust LOESS methods are more flexible than robust linear models, a model that is accurately fit to the LEA structure results in the same expected residual structure as with robust linear models: positive and negative residuals scattered around zero in the LEA zone, and positive, possibly large residuals in the GEA zones. A similar approach using a cutoff value can be employed to distinguish between “large” residual values and reasonable ones. Since non-parametric fits offer a closer fit over a large amount of data, the cutoff for separation will be lower. A cutoff that performs well on the Hamby set 44 is twice the median absolute deviation ($2 \times MAD$).

Shoulder location predictions are calculated for each profile in the following manner:

1. Fit a robust LOESS model with a span of 1 to the averaged profile. This can be fit using the ‘locfit.robust’ function in the ‘locfit’ package in R.
2. Calculate a residual value for each data point on the profile.
3. Calculate the median absolute deviation (MAD) for the profile.
4. Remove all data points on the profile whose absolute residual value is greater than $2 \times MAD$.
5. Identify the range of the remaining Y values - these are the predicted shoulder locations for that profile.

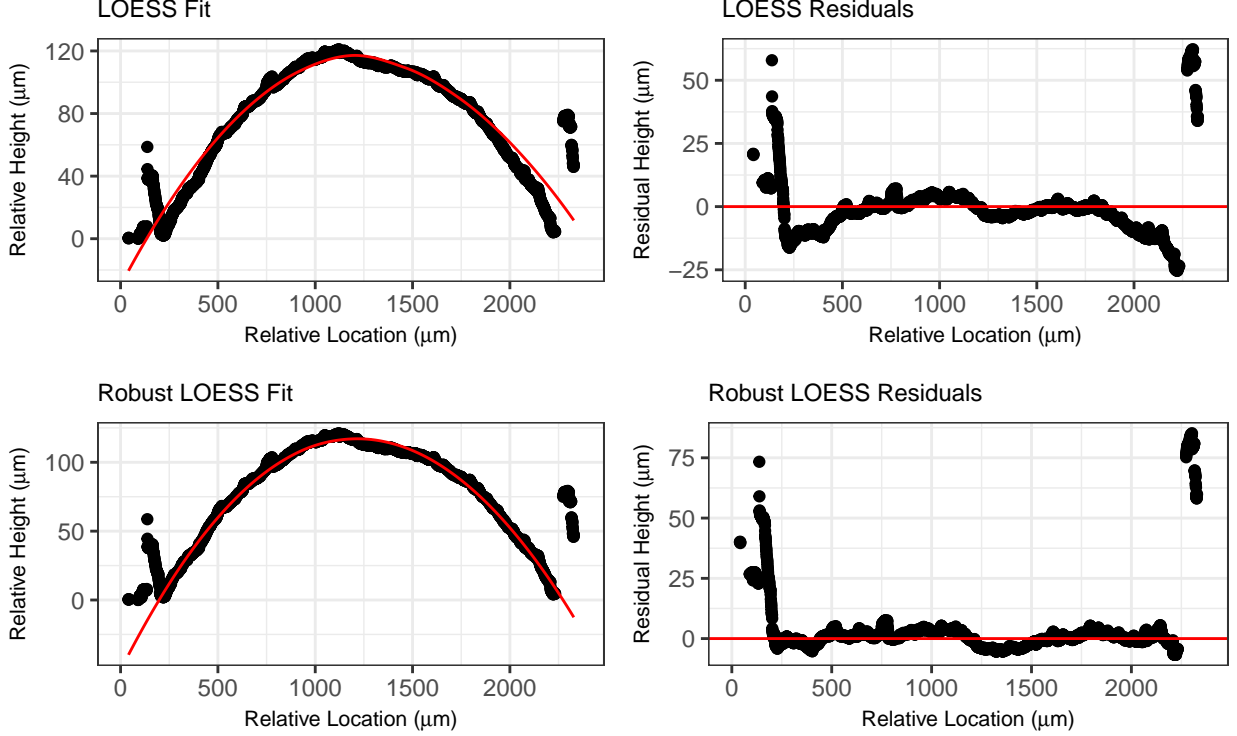


Figure 7: Example of a LOESS model fit and residuals (top) compared to a robust LOESS model fit and residuals (bottom) for a single profile. The robust model is again able to more effectively capture the curved structure of the LEA without being influenced by the GEA.

4 Results

In order to assess the accuracy of the two alternative models based on a quantitative measure for their overall performance of predictions, we first manually identified “ground truth” shoulder locations for each of the 208 profiles in Hamby set 44. on which data? tie it back to the data section.

the next couple of paragraphs up to XXX need more work. You are going chronologically through the explanation - that puts too much emphasis on things we decided not to do. Come in from the back, i.e. define the measure used first, then go into some explanation.

Using ground truth shoulder locations, we calculate an "area of misidentification", the area in microns of a profile which is considered incorrectly identified by the method. This metric is calculated separately for the left shoulder location as:

$$\hat{A}_{jL} = \left| \sum_{z_{ij} \in \tilde{Z}_{jL}} (z_{ij} - \hat{z}_{ij}) \times 0.645 \mu m \right|,$$

where \tilde{Z}_{jL} is the set of points in profile j that fall between the predicted left shoulder location and ground truth left shoulder location, and \hat{z}_{ij} is the predicted height value at location i from the robust LOESS fit to profile j .

The analogous area is calculated for the right shoulder location as:

$$\hat{A}_{jR} = \left| \sum_{z_{ij} \in \tilde{Z}_{jR}} (z_{ij} - \hat{z}_{ij}) \times 0.645 \mu m \right|,$$

where \tilde{Z}_{jR} is the set of points in profile j that fall between the predicted right shoulder location and ground truth right shoulder location, and \hat{z}_{ij} is again the predicted height value at location i from the robust LOESS fit to profile j .

Both the left and right areas of misidentification are thus in terms of microns and represent the area of loss we incur from incorrectly identifying a shoulder location.

The quantification of results as an area is preferable to a distance metric as it captures not only the width of profile area that is misidentified, but also the relative heights of the data. Larger areas of misidentification indicate larger portions of the GEA remain included in a profile, and thus signal an area which is more likely to have influence on an extracted signature. Smaller areas of misidentification indicate minimal loss is incurred, and these areas will have minimal effect on an extracted signature.

The residual heights used in the calculation of \hat{A}_{jL} and \hat{A}_{jR} , denoted as $(z_{ij} - \hat{z}_{ij})$, are residuals resulting from a robust LOESS fit. These residuals are used for quantification of results regardless of which method is being assessed due to the fact that robust LOESS most reliably approximates the curved shape of the bullet land. The pattern of residual values is most reliable using robust LOESS and thus leads to the most interpretable areas of misidentification.

An area of misidentification was calculated separately for the left hand side and right hand side predictions for each profile in the data set. This was calculated for the Robust Linear Model and Robust LOESS methods, as well as the Rollapply method suggested in Hare et al. [2017].

How is the section above now? Would replace everything below until XXX.

The numerical comparison of predicted and manually identified locations can be tricky; distance metrics alone do not suffice to represent the true character of a prediction’s accuracy. For example, a predicted shoulder location that falls 10 data points away from the manually identified shoulder location could be caused by noise in the data, missing data points, or simply the scale of the data. Note that a span of 10 data points represents only 6.45 microns in physical space. Alternatively, a distance of 10 points could indeed be part of the groove engraved area, and thus being incorrectly identified could potentially cause problems in subsequent analyses.

A more suitable measure is to investigate the residual values resulting from the robust LOESS model that fall in the range spanned by the predicted and manually identified shoulder location. This method penalizes shoulder location predictions that are too far out to the side and leave GEA data in the main structure.

Because the robust LOESS most reliably approximates the curved shape of the bullet land due to its flexibility, we want to use residual values resulting from that model to assess final performance of all methods. Residual values from the GEA will not necessarily be uniformly large, but are expected to be positive as their structure and the modeling technique dictate that they would fall above the fitted line from robust LOESS.

With positive residuals in the GEA, even a 10-point difference can quickly add to a large residual sum. However, a 10-point difference within the land engraved area will be balanced out by the presence of both positive and negative residual values and remain closer to zero.

For this reason, gathering the sum of residuals between the predicted location and the manually identified location is appropriate. This residual sum is referred to as an “inaccuracy score” for which higher values indicate a higher level of inaccuracy. An inaccuracy score was calculated separately for the left hand side and right hand side predictions for each profile in the data set. This was calculated for the Robust Linear Model and Robust LOESS methods, as well as the Rollapply method suggested in Hare et al. [2017].

XXX

Of interest are the distributions of these [areas of misidentification](#) across all 208 lands used in the study (see Figure 8). A distribution that has a smaller spread and is close to zero is ideal; this suggests many

of the predicted shoulder locations are very close to the manually identified locations, and predictions are removing many of the outlying GEA points. A distribution with a wider spread or many high, outlying [areas of misidentification](#) suggests a greater degree of uncertainty and inaccuracy for a particular method.

The raw distributions can be difficult to visually compare, so another way to inspect the results is to place areas of misidentification into categories: satisfactory, borderline, unsatisfactory. Scores under 100 are satisfactory, scores between 100 and 1000 are borderline, and scores above 1000 are unsatisfactory (see Figure 9). Unsatisfactory cases are the most likely to cause mistakes in subsequent analyses.

It is important to note that different results are expected for the left and right shoulder locations. Within Hamby set 44, almost all scans have a well-defined left groove. Left here is defined as visually left on the scan; this is the side the scan begins on, so a well-defined distinction between GEA and LEA is expected. Often, a less clear distinction is seen on the right side of the scan, with sometimes no apparent shoulder location visible. For this reason it is preferable to separate the left and right for visual inspection of results; a method may excel on one side but fall short on another.

5 Conclusions

Both the robust linear model and robust LOESS approaches outperform currently implemented solutions based on data smoothers. Of the two, the robust LOESS approach clearly outperforms the robust linear model. This hierarchy of performance is well within expectation given the strength of robust approaches in general as well as the flexibility of LOESS applied to this data type. Robust LOESS also readily handles variation introduced in the process of translating the physical bullet into a 3D object. If there is too much variability in how the bullet is placed relative to the plane of reference on the microscope, profiles can have tilted shapes relative to the x-axis which a quadratic linear model would fail to address. In these situations, LOESS excels.

While the cutoff values presented work well on Hamby set 44, additional validation will need to be implemented on a variety of bullet types. Depth of striae, physical size of bullet due to caliber, and non-traditional rifling techniques may require alterations to this cutoff value. In addition, a study of the effect of implementing a robust LOESS data pre-processing strategy on overall automated image-analysis methods will need to be addressed. Due to increased accuracy of predicted shoulder locations, the authors expect an increase in accuracy in bullet matching algorithms. However, this will need to be validated on a variety of data sets prior to implementation without human intervention in the automated process.

6 References

References

- AFTE Glossary. Theory of identification as it relates to toolmarks. *AFTE Journal*, 30(1):86–88, 1998.
- Benjamin Bachrach. Development of a 3d-based automated firearms evidence comparison system. *Journal of Forensic Sciences*, 47(6):1253–1264, 2002.
- Alfred A. Biasotti. A statistical study of the individual characteristics of fired bullets. *Journal of Forensic Sciences*, 4(1):34–50, 1959.
- Wei Chu, T. Song, J. Vorburger, J. Yen, S. Ballou, and B. Bacharach. Pilot study of automated bullet signature identification based on topography measurements and correlations. *Journal of Forensic Sciences*, 55(2):341–47, 2010.
- Wei Chu, Robert M Thompson, John Song, and Theodore V Vorburger. Automatic identification of bullet signatures based on consecutive matching striae (cms) criteria. *Forensic Science International*, 231(1-3): 137–41, 2013.

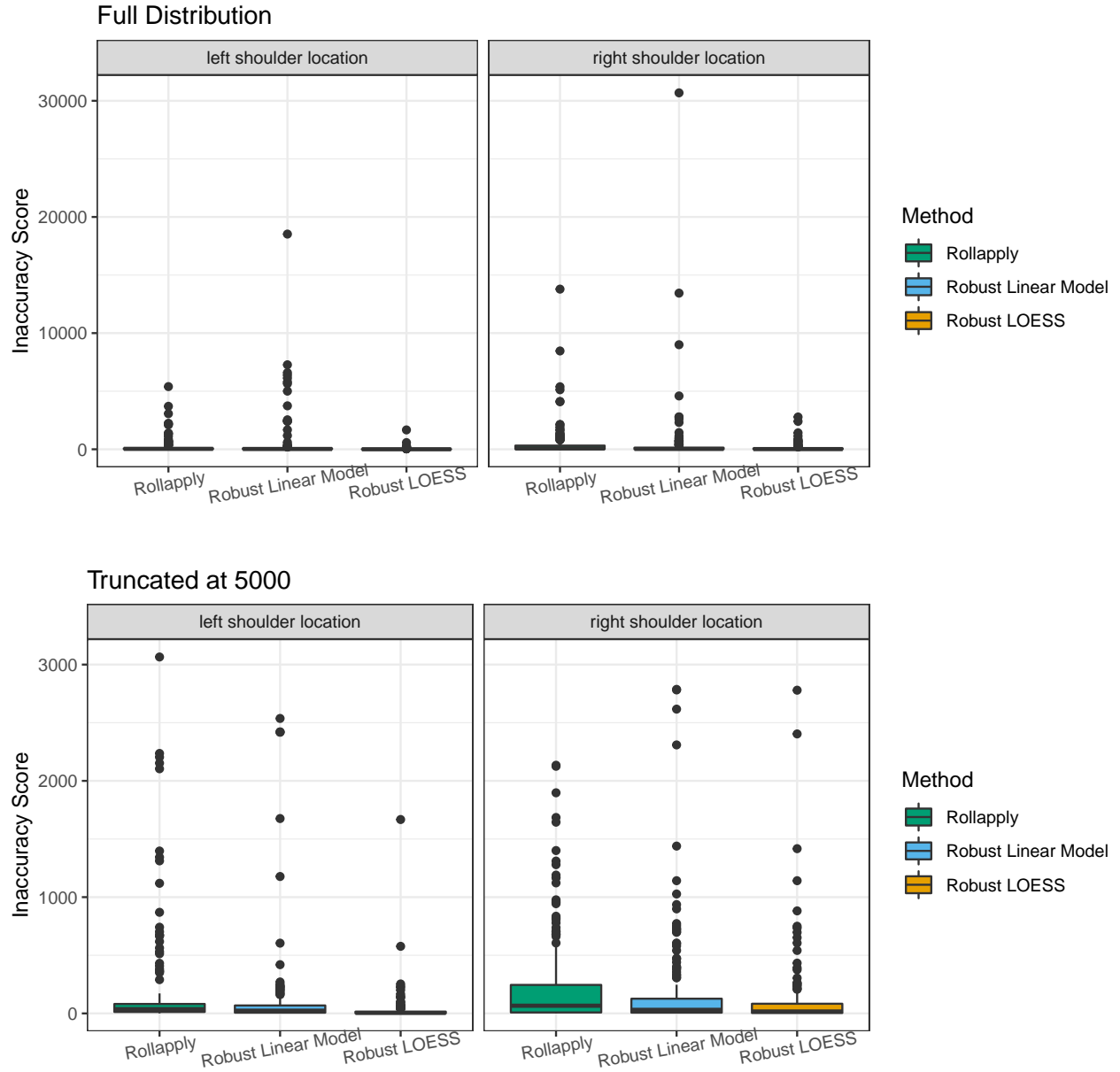


Figure 8: Distribution of areas of misidentification for data smoothing method, robust linear model method, and robust LOESS method, separated by left and right shoulder locations. A tight distribution with few high values indicates good performance across the LEAs in the data set.

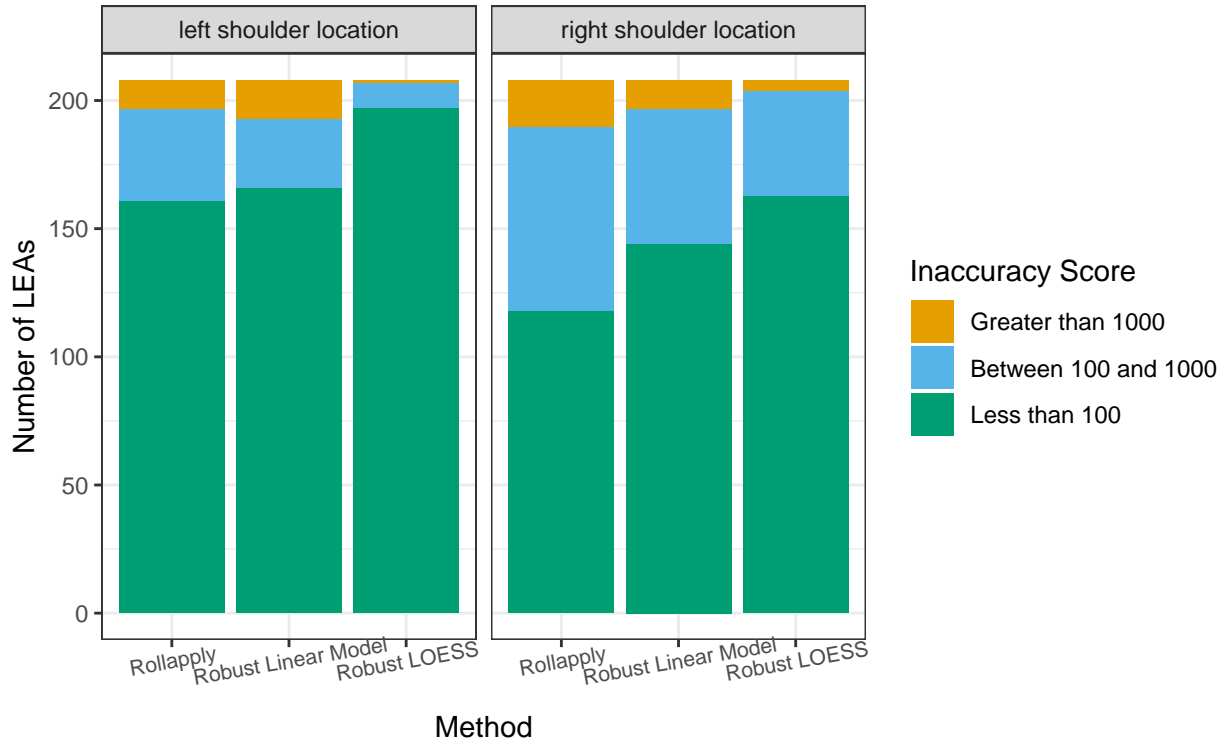


Figure 9: Distribution of areas of misidentification for data smoothing method, robust linear model method, and robust LOESS method, separated by left and right shoulder locations. Areas of misidentification are placed into three categories: less than 100 microns (satisfactory), between 100 and 1000 microns, and greater than 1000 microns. A larger proportion of areas of misidentification under 100 microns indicates good performance across LEAs in the data set.

- William S. Cleveland. Robust locally weighted regression and smoothing scatterplots. Journal of the American Statistical Association, 74(368):829–836, 1979.
- J. De Kinder and M. Bonifanti. Automated comparison of bullet striations based on 3d topography. Forensic Science International, 101:85–93, 1999.
- J. De Kinder, P. Prevot, M. Pirlot, and B. Nys. Surface topology of bullet striations: an innovating technique. AFTE Journal, 30(2):294–299, 1998.
- James E. Hamby, David J. Brundage, and James W. Thorpe. The identification of bullets fired from 10 consecutively rifled 9mm ruger pistol barrels: A research project involving 507 participants from 20 countries. AFTE Journal, 41(2):99–110, 2009.
- Eric Hare, Heike Hofmann, and Alicia Carriquiry. Automatic matching of bullet land impressions. The Annals of Applied Statistics, 11:2332–2356, 12 2017.
- ISO 5436-2:2012(en). Geometrical product specifications (GPS) – Surface texture: Profile method; Measurement standards – Part 2: Software measurement standards. Standard, International Organization for Standardization, Geneva, CH, 2012.
- L. Ma, J. Song, E. Whitenton, A. Zheng, T. Vorburger, and J. Zhou. Nist bullet signature measurement system for rm (reference material) 8240 standard bullets. Journal of Forensic Sciences, 49(4):649–59, 2004.